Photodiagnosis and Photodynamic Therapy 43 (2023) 103724

Contents lists available at ScienceDirect

Photodiagnosis and Photodynamic Therapy

journal homepage: www.elsevier.com/locate/pdpdt

Impact of obesity on peripapillary choroidal thickness, macular choroidal thickness, and lamina cribrosa morphology

Sumeyra Koprubasi [a,*], Erkan Bulut [b]

[a] Department of Ophthalmology, Sancaktepe Sehit Prof. Dr. Ilhan Varank Training and Research Hospital, Istanbul, Turkey
[b] Department of Opticianry, Vocational School of Health Services, Istanbul Gelisim University, Istanbul, Turkey

ARTICLE INFO

Keywords:
Peripapillary choroidal thickness
Macular choroidal thickness
Bruch's membrane opening
Lamina cribrosa thickness
Lamina cribrosa depth
OCT

ABSTRACT

Background: Obesity is known to be a significant risk factor for many ocular diseases. In order to understand the mechanism of obesity-related ocular diseases, we examined the lamina cribrosa morphology, peripapillary choroidal thickness (PPCT), and macular choroidal thickness (MCT) in obese women using optical coherence tomography (OCT).

Methods: This comparative cross-sectional study included the right eyes of 72 obese women and 63 healthy women classified based on body mass index (BMI). Each participant underwent a thorough ophthalmological examination and enhanced depth (EDI) OCT imaging, including measurements of PPCT from a total of 12 regions, MCT from a total of 7 regions, Bruch's membrane opening (BMO), lamina cribrosa thickness (LCT), lamina cribrosa depth (LCD), intraocular pressure (IOP), and central corneal thickness (CCT).

Results: The mean age and BMI of the obese group were 32.36±7.38 years and 35.11±4.39 kg/m^2, while those of the control group were 31.64±7.78 years and 20.88±1.72 kg/m^2 ($p = 0.658$, and $p<0.001$, respectively). PPCT N1000, PPCT N1500, PPCT S1500, and PPCT T1500 were statistically significantly thinner in the obese group than the control group (p values were 0.039, 0.012, 0.027, and 0.036, respectively). IOP and CCT were significantly higher in the obese group than the control group ($p = 0.016$, and $p = 0.019$, respectively). There was no statistically significant difference between the two groups in terms of MCT, BMO, LCT, and LCD.

Conclusion: We discovered thinning in the PPCT, which indicates microvascular abnormalities in the optic disc head. Microvascular alteration in the peripapillary region may be a potential initial event in the pathogenesis of several obesity-related ocular diseases, especially glaucoma.

1. Introduction

Obesity is a significant public health issue that has been considered a sort of pandemic by the World Health Organization due to its rapidly increasing prevalence [1]. By 2025, the prevalence of obesity is projected to be 21% among females and 18% among males [2]. Obesity is a major public health issue since it raises the development and progression risk of numerous serious systemic diseases, including diabetes mellitus, hypertension, coronary artery disease, and obstructive sleep apnea syndrome [3–5]. Previous research has linked obesity to a number of ocular disorders, including impaired vision, glaucoma, age-related macular degeneration (AMD), cataract, and diabetic retinopathy [6–8]. The increase in adipose tissue reduces the production of adiponectin, which causes insulin resistance and contributes to the

Abbreviations: AMD, age-related macular degeneration; ACD, anterior chamber depth; AXL, axial length; BMI, body mass index; BMO, Bruch's membrane opening; CCT, central corneal thickness; DBP, diastolic blood pressure; GCL, ganglion cell layer; IPL, inner plexiform layer; ICC, intraclass correlation coefficient; IOP, intraocular pressure; LC, lamina cribrosa; LCD, lamina cribrosa depth; LCT, lamina cribrosa thickness; MCT, macular choroidal thickness; MCT TX, macular choroidal thickness at a distance of X micrometers in the temporal region; MCT NX, macular choroidal thickness at a distance of X micrometers in the nasal region; ONH, optic nerve head; OCT, optical coherence tomography; PPCT, peripapillary choroidal thickness; PPCT IX, peripapillary choroidal thickness at a distance of X micrometers in the inferior region; PPCT NX, peripapillary choroidal thickness at a distance of X micrometers in the nasal region; PPCT SX, peripapillary choroidal thickness at a distance of X micrometers in the superior region; PPCT TX, peripapillary choroidal thickness at a distance of X micrometers in the temporal region; RNFLT, retinal nerve fiber layer thickness; RPE, retinal pigment epithelium; SFCT, subfoveal choroidal thickness; SeQ, spherical equivalent; SBP, systolic blood pressure (SBP).

* Corresponding author at: Department of Ophthalmology, Sancaktepe Şehit Prof. Dr. Ilhan Varank Training and Research Hospital., Emek Mah. Namık Kemal Cad. No:54, 34785 Sancaktepe, Istanbul, Turkey.

E-mail addresses: smyragca@hotmail.com, drsumeyrakoprubasi@gmail.com (S. Koprubasi).

https://doi.org/10.1016/j.pdpdt.2023.103724
Received 20 June 2023; Received in revised form 24 July 2023; Accepted 24 July 2023
Available online 29 July 2023

development of all diabetic complications, including diabetic retinopathy [6]. BMI and abdominal obesity are considered independent risk factors for senile cataract [7]. Obesity has also been identified as an important avoidable cause of AMD. BMI has a significant positive connection with neovascular AMD and geographic atrophy [8]. It is well known that obesity raises intraocular pressure (IOP) and is an important risk factor for the development of glaucoma [9–11]. Although the pathogenesis of the relationship between obesity and ocular diseases has not been fully defined yet, endothelial dysfunction and vascular damage due to oxidative stress are considered to be the main reasons [12,13].

Microvascular perfusion dysfunction in the optic nerve head (ONH) is considered to be the most important factor in the pathogenesis of glaucoma [14,15]. The blood circulation of ONH is provided by branches of short posterior ciliary vessels in the peripapillary choroidal area [l4]. The thinning of the peripapillary choroidal thickness (PPCT) indicates a microvascular impairment in ONH. Another significant theory for the pathogenesis of glaucoma is axonal damage due to the deterioration in the structure of the lamina cribrosa (LC) [16,17]. The LC is a fibrous network structure that surrounds and supports the ONH. LC have two crucial functions for the ONH. Firstly, the collagen fibers in LC structure provide a protective sheath around the ONH, preserving its form and strength [16]. Secondly, LC creates an aperture for the bundle of retinal ganglion cell axons to gather and exit the globe, allowing visual information to be conveyed to the brain via the middle cranial fossa [17]. It has been reported that the thinning and displacement of the LC due to the structural abnormality or exposure to stress by elevated IOP causes axonal damage and leads to the development of glaucoma [16, 17]. Bruch's membrane opening (BMO) rim width is also a quantitative measurement that offers an anatomically accurate evaluation of the neuroretinal rim's outer boundaries in the ONH. It has been reported that BMO is a more sensitive parameter than retinal nerve fiber layer thickness (RNFLT) in detecting early glaucomatous changes [18].

In this study, we assessed PPCT, macular choroidal thickness (MCT), BMO, lamina cribrosa thickness (LCT), and lamina cribrosa depth (LCD) in obese women based on both the vascular and laminar theories of glaucoma. Therefore, we aimed to investigate the mechanism underlying the association between obesity and other ocular diseases, especially glaucoma.

2. Materials and methods

2.1. Ethical statement

This cross-sectional comparative investigation was conducted in accordance with the Declaration of Helsinki and was approved by the ethics committee of Biruni University, Istanbul, Turkey. Before the enrollment, written informed consent was obtained from each participant.

2.2. Subjects

The study included 72 obese women and 63 normal-weight healthy women who underwent routine control at the ophthalmology department of Beylikduzu State Hospital between 2020 and 2022. Body mass index (BMI) was used to determine and classify obesity. The BMI was calculated by dividing the subject's weight in kilograms by their height in meters squared (kg/m^2). A BMI of 18.5–24.9 kg/m^2 is regarded as normal, 25.0–29.9 kg/m^2 as overweight, and 30.0 kg/m^2 or above as obese [19]. Women over the age of 18 with a BMI of 30 kg/m^2 or more were included in the obese group, whereas women over the age of 18 with a BMI of 25 kg/m^2 or less were included in the control group.

The hospital's data recording system verified the thorough medical histories provided by each subject. Subjects were excluded from the study based on the following criteria: Any systemic diseases, such as diabetes mellitus, hypertension, or coronary artery disease; any ocular diseases; a history of ocular surgery or laser therapy; greater than 2D refractive error; a history of medication usage, smoking, or alcohol intake; insufficient OCT imaging with a signal strength below 8/10 and signal-to-noise ratio (SNR) below 20 dB.

2.3. Physical and ophthalmological examination

A general physical examination was performed on each subject, including measurements of height, weight, BMI, systolic blood pressure (SBP), and diastolic blood pressure (DBP). Following the rest period, blood pressure was automatically assessed three times within a 15-minute interval, and the measurements were averaged.

Each subject underwent an entire ophtalmological examination, including assessments of best-corrected visual acuity, spherical equivalent (SeQ), slit-lamb biomicroscopy, IOP, central corneal thickness (CCT), axial length (AXL), anterior chamber depth (ACD), and optical coherence tomography (OCT) imaging. Autokeratorefractometry (Topcon KR-800, Topcon Medical Systems, Inc., Fukuoka, Japan), Goldmann applanation tonometry, non-contact tonopachymetry (NT-530P, Nidek Co., Gamagori, Japan), and optic biometry (Nidek Axial Length-Scan, Nidek CO., Gamagori, Japan) were used for the measurements. The right eyes of each subject were examined and compared in the study.

Spectralis OCT (Cirrus HD OCT, Carl Zeiss Meditec, Dublin, CA, USA) was used for posterior segment imaging. The thicknesses of the ganglion cell layer (GCL) and the inner plexiform layer (IPL) were assessed using the macular cube procedure of OCT. The RNFLT and cup-to-disc ratio assessments were performed using the OCT Disc Cube 200 × 200 procedure. The average, superior, inferior, nasal, and temporal RNFLT were measured.

The LCT, LCD, and BMO measurements were made on horizontal scans passing through the ONH using the HD 1-line-edi procedure of OCT based on previous research [20,21] (Fig. 1). During imaging, the device was positioned closer to the eye to better visualize the deep components of the posterior ocular region by shifting the zero reference line further back. Since the LC structure is smoother in the horizontal plane, horizontal scans were used. In order to get more accurate measurements of the W-shaped LC, measurements were made in three sections, superior, middle, and inferior scans of the ONH, and their averages were calculated [22,23]. The distance between the two end points of Bruch's membrane in the nasal and temporal ONH was measured for the BMO assessment. The distance between the BMO and the anterior edge of the LC was measured for the LCD assessment. The LCT was measured as the distance between the front and back edges of the LC when hyperreflectivity is greatest in the bottom region of the ONH. All images evaluated in the study were high-quality images with a SNR above 20 dB [24]. The images with signal strength below 8\10 and SNR below 20 dB were not included in the study. All measurements were made in duplicate by two experienced ophthalmologists in different sessions, and the averages of their measurements were used for analysis.

MCT measurements were performed using a high-quality image of the macula using the HD 1-line-edi procedure of OCT. MCT was measured at seven regions, including the center of the fovea, nasal, and temporal regions at 500 μm, 1000 μm, and 1500 μm distance from the fovea (Fig. 2). Vertical and horizontal scans crossing through the ONH center were utilized to assess PPCT using the OCT HD 5-Line Raster-Edi procedure. PPCT measurements were performed at the superior, inferior, nasal, and temporal regions at 500 μm, 1000 μm, and 1500 μm distances from the ONH border, for a total of 12 regions (Fig. 3). All MCT and PPCT measurements were performed manually by two experienced ophthalmologists (EB, SK) on 100% magnification images, measuring the vertical distance between the retinal pigment epithelium (RPE) border above and the chorioscleral border below. Interobserver compatibility analysis of the CT measurements of both ophthalmologists was performed, and the averages of the two observers' measurements were used in further analysis. All examinations were performed on each subject between 9:00 a.m. and 11:00 a.m. to avoid diurnal fluctuations.

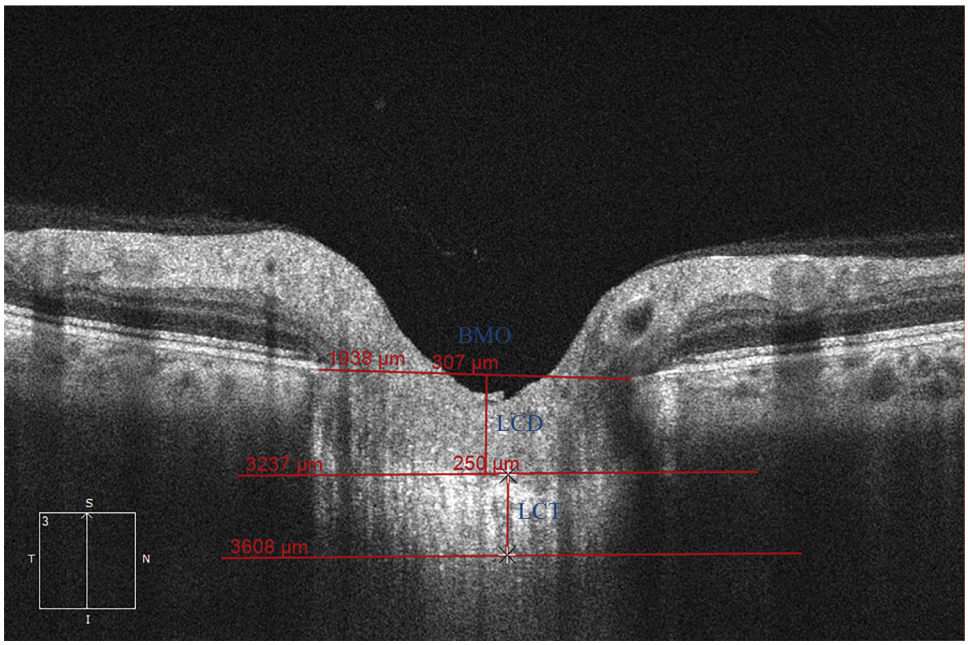

Fig. 1. Lamina cribrosa measurements on OCT scan.
BMO: Bruch's membrane opening; LCD: lamina cribrosa depth; LCT: lamina cribrosa thickness. BMO was measured as the distance between the two end points of Bruch's membrane in the nasal and temporal regions of optic nerve head. LCD was measured as the distance between the BMO and the anterior edge of lamina cribrosa. LCT was measured as the distance between the front and back edges of lamina cribrosa when hyperreflectivity is highest in the bottom region of the optic nerve head.

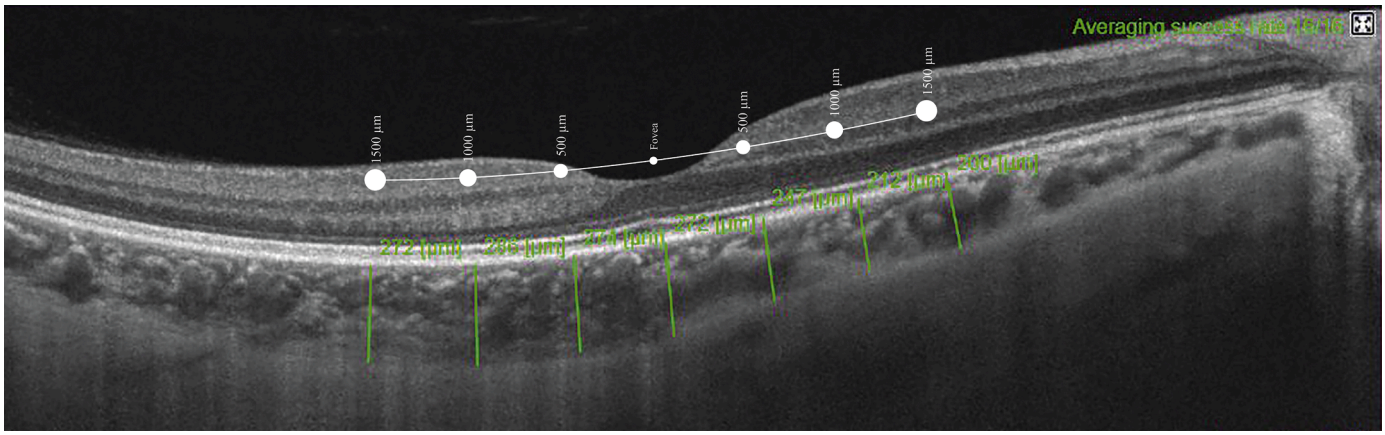

Fig. 2. Macular choroidal thickness measurements on OCT scan.
Macular choroidal thicknesses were assessed at seven regions, including the center of the fovea, nasal, and temporal regions at 500 µm, 1000 µm, and 1500 µm distance from the fovea. The vertical distance between the retinal pigment epithelium border above and the chorioscleral border below was measured for each region.

2.4. Statistical analysis

All statistical analyses were performed using IBM SPSS for Windows version 23.0 (Statistical Package for Social Sciences, Chicago, Illinois, USA). The Shapiro-Wilk test was used to examine the normality of numeric variables. The variables with a normal distribution were analyzed using an independent sample Student's *t*-test and described as mean±standard deviation, whereas variables with a non-normal distribution were analyzed using the Mann-Whitney U test and expressed as median (25–75%). The categorical variables were assessed using the chi-squared test and described as numbers and percentages. The intraclass correlation coefficient (ICC) test was performed for interobserver agreement analysis. The Pearson correlation analysis was performed to examine the link between BMI and other variables. $P<0.05$ was considered statistically significant.

3. Results

The study group included 72 obese women with a BMI of 35.11 ±4.39 kg/m^2, while the control group included 63 women of normal weight with a BMI of 20.88±1.72 kg/m^2 ($p<0.001$). The mean age of the obese group was 32.36±7.38 years, whereas 31.64±7.78 years in the control group, without a statistically significant difference ($p>0.05$). The demographic and clinical data of both groups were displayed in Table 1. There was no statistically significant difference between the two groups in terms of SeQ, ACD, AXL, SBP, and DBP ($p>0.05$). However, it was remarkable that IOP and CCT were significantly higher in the obese group than the control group (p values were 0.016, and 0.019, respectively).

Interobserver agreement of choroidal measurements were displayed in Table 2. The calculated ICC value for each CT measurement was greater than 0.90. The agreement between the observers was at a perfect level for each measurement.

The comparison of OCT measurements between the two groups were displayed in Table 3. There was no statistically significant difference between the two groups in terms of BMO, LCD, LCT, RNFLT, GCC+IPL, and macular thicknesses ($p>0.05$). It was noteworthy that PPCT N1000, PPCT N1500, PPCT S1500, and PPCT T1500 were statistically significantly thinner in the obese group than the control group (p values were 0.039, 0.012, 0.027, and 0.036, respectively). Although not statistically

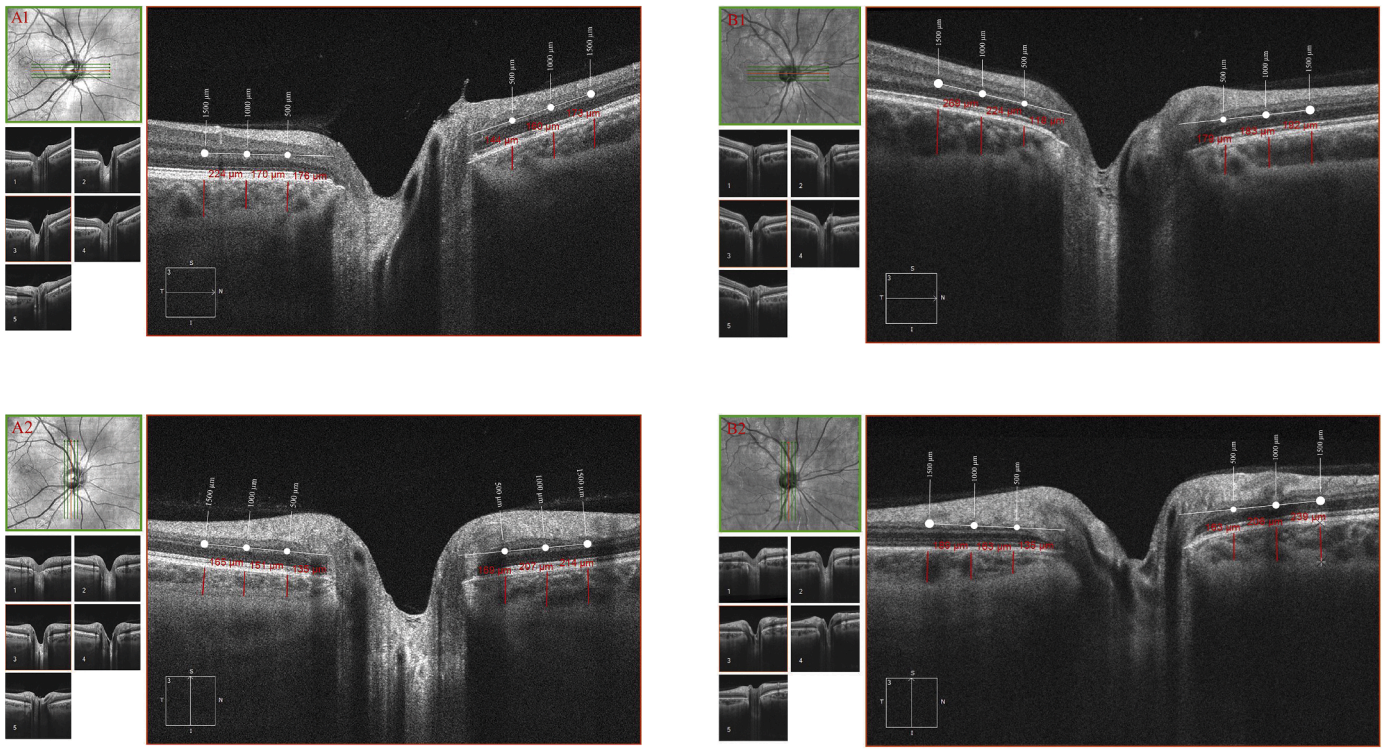

Fig. 3. Peripapillary choroidal thickness measurements on OCT scan.
A1: Peripapillary choroidal thickness measurements on horizontal OCT scan of obese subject. The measurements were performed at 500 μm, 1000 μm, and 1500 μm distance from the boundary of optic nerve head in temporal and nasal regions.A2: Peripapillary choroidal thickness measurements on vertical OCT scan of obese subject. The measurements were performed at 500 μm, 1000 μm, and 1500 μm distance from the boundary of optic nerve head in superior and inferior regions. B1: Peripapillary choroidal thickness measurements on horizontal OCT scan of normal-weighted control subject. The measurements were performed at 500 μm, 1000 μm, and 1500 μm distance from the boundary of optic nerve head in temporal and nasal regions. B2: Peripapillary choroidal thickness measurements on vertical OCT scan of normal-weighted control subject. The measurements were performed at 500 μm, 1000 μm, and 1500 μm distance from the boundary of optic nerve head in superior and inferior regions. Notable is the fact that the peripapillary choroidal thickness measurements of the obese subject were thinner than the control subject, particularly at 1000 μm and 1500 μm distances.

Table 1
Comparison of demographic and clinical data between the obese and the control group.

	Obese group $N = 72$	Control group $N = 63$	Total $N = 135$	P
Age (years)	32.36±7.38	31.64±7.78	31.94±7.42	0.658
BMI (kg/m^2)	35.23±4.46	20.88±1.72	29.66±7.86	<0.001*
SeQ	−0.34±0.92	−0.42±0.86	−0.39±0.84	0.778
SBP (mmHg)	122.54±13.74	116.65±21.82	120.24±16.35	0.088
DBP (mmHg)	73.26±8.72	69.98±7.24	71.82±8.33	0.082
ACD (mm)	3.52±0.44	3.58±0.58	3.52±0.52	0.662
AXL (mm)	23.42±0.81	23.59±0.86	23.52±0.74	0.789
IOP (mmHg)	16.84±2.62	15.04±3.5	16.24±3.36	0.016*
CCT (μm)	545.56±32.93	528.28±41.58	538.44±36.34	0.019*

BMI: body mass index; SeQ: sferical equivalent; SBP: systolic arterial pressure; DBP: diastolic arterial pressure; ACD: anterior chamber depth; AXL: axial length; IOP: intraocular pressure; CCT: central corneal thickness.
Comparisons of the two groups were evaluated through Student t-test and expressed as mean±sd. $P<0.05$: statistically significant.

significant, PPCT I1000 and PPCT T1000 were also observed to be slightly thinner in the obese group (both p values were 0.066). There was no statistically significant difference between the two groups in terms of any MCT measurements ($p>0.05$).

The correlation analysis of BMI with other parameters were displayed in Table 4. A statistically significant negative correlation was found between BMI and PPCT N1000, PPCT N1500, and PPCT S1500. It was notable that BMI had a significant positive correlation with SBP, and DBP.

Table 2
Interobserver agreement of choroidal measurements.

	ICC (95% CI)
PPCT T500	0.903 (0.858–0.934)
PPCT T1000	0.900 (0.770–0.910)
PPCT T1500	0.964 (0.947–0.976)
PPCT N500	0.947 (0.921–0.964)
PPCT N1000	0.965 (0.947–0.976)
PPCT N1500	0.966 (0.948–0.977)
PPCT S500	0.946 (0.920–0.964)
PPCT S1000	0.945 (0.900–0.970)
PPCT S1500	0.957 (0.936–0.971)
PPCT I500	0.949 (0.924–0.966)
PPCT I1000	0.932 (0.899–0.954)
PPCT I1500	0.933 (0.901–0.955)
SFCT	0.948 (0.922–0.965)
MCT T500	0.974 (0.960–0.982)
MCT T1000	0.930 (0.897–0.953)
MCT T1500	0.901 (0.856–0.933)
MCT N500	0.961 (0.943–0.974)
MCT N1000	0.939 (0.910–0.959)
MCT N1500	0.941 (0.912–0.960)

ICC: Intraclass correlation coefficient; CI: confidence interval; PPCT T: temporal peripapillary choroidal thickness, PPCT N: nasal peripapillary choroidal thickness; PPCT S: superior peripapillary choroidal thickness; PPCT I: inferior peripapillary choroidal thickness; SFCT: subfoveal choroidal thickness; MCT T: temporal macular choroidal thickness; MCT N: nasal macular choroidal thickness.

Table 3
Comparison of OCT parameters between the obese and the control group.

	Obese group $N = 72$	Control group $N = 63$	Total $N = 135$	P
GCL+IPL thickness (μm)	83 [56–97]	83.50 [65–91]	84 [56–309]	0.672
Macular thickness (μm)	245 [87–308]	244 [216–300]	244 [87–308]	0.459
average c/d (%)	0.42±0.17	0.42±0.18	0.42±0.18	0.988
vertical c/d (%)	0.39±0.17	0.41±0.17	0.4±0.17	0.743
superior RNFLT (μm)	120.1±14.37	121.33 ±17.02	120.57 ±15.35	0.707
nasal RNFLT (μm)	74.03±12.43	76.03±10.87	74.79±11.85	0.429
inferior RNFLT (μm)	124.36±17.6	130.06 ±12.48	126.52 ±16.02	0.093
temporal RNFLT (μm)	69.69±17.48	68±8.72	69.05±14.75	0.590
average RNFLT (μm)	96.59±9.33	98.97±8.84	97.49±9.17	0.222
BMO (μm)	1670.88 ±176.46	1725.83 ±156.5	1692.15 ±170.28	0.130
LCD (μm)	383.1±97.63	352.3±92.84	371.86 ±96.32	0.225
LCT (μm)	237.58±30.7	223.3±50.79	232.37 ±39.45	0.169
PPCT T500 (μm)	152.48 ±46.94	151.1±46.72	151.96 ±46.61	0.889
PPCT T1000 (μm)	291.12±68	306.28 ±66.55	296.86±67.5	0.291
PPCT T1500 (μm)	303.78 ±73.67	328.47 ±66.01	313.14 ±71.53	0.103
PPCT N500 (μm)	168.82 ±64.81	190.78±67.3	177.14 ±66.28	0.118
PPCT N1000 (μm)	196.06 ±68.19	227.61 ±75.69	208.02 ±72.38	0.039*
PPCT N1500 (μm)	209.66 ±66.92	247.68 ±75.83	224.07 ±72.45	0.012*
PPCT S500 (μm)	173.86 ±60.06	181.25 ±69.17	176.66±63.4	0.584
PPCT S1000 (μm)	290.11 ±67.69	311.79 ±62.71	298.33 ±66.36	0.123
PPCT S1500 (μm)	223.26 ±61.27	254.63 ±73.26	235.15 ±67.44	0.027*
PPCT I500 (μm)	142,31 ±39,72	140,11 ±49,21	141,47 ±43,31	0,812
PPCT I1000 (μm)	361.11 ±82.89	391.78 ±68.75	372.73 ±78.88	0.066
PPCT I1500 (μm)	178.69 ±51.78	185.65 ±64.34	181.33 ±56.63	0.564
SFCT (μm)	359.74 ±82.86	378.86 ±71.78	366.92 ±79.46	0.272
MCT T500 (μm)	366.21 ±86.39	394.93 ±71.83	377.09 ±81.99	0.098
MCT T1000 (μm)	361.11 ±82.89	391.78 ±68.75	372.73 ±78.88	0.066
MCT T1500 (μm)	349.66 ±80.65	384.14 ±69.24	362.73 ±77.98	0.036*
MCT N500 (μm)	359.56 ±84.82	381.16 ±72.67	367.75 ±80.72	0.208
MCT N1000 (μm)	328.26 ±83.48	338.78 ±82.43	332.25±82.8	0.551
MCT N1500 (μm)	302.77 ±86.17	307.71 ±83.71	304.64 ±84.83	0.785

OCT: optical coherence tomography; GCL+IPL: ganglion cell layer+inner plexiform layer; RNFLT: retinal nerve fiber layer thickness; BMO: Bruch's membrane opening; LCD: lamina cribrosa depth; LCT: lamina cribrosa thickness; PPCT T: temporal peripapillary choroidal thickness; PPCT N: nasal peripapillary choroidal thickness; PPCT S: superior peripapillary choroidal thickness; PPCT I: inferior peripapillary choroidal thickness; SFCT: subfoveal choroidal thickness, MCT T: temporal macular choroidal thickness; MCT N: nasal macular choroidal thickness.

Mean±sd for normal distributed variables, median [min-max] for non-normal distributed variables.

Comparisons between the obese and the control groups were evaluated through *t*-test or Mann Whitney U test. $P<0.05$: statistically significant.

Table 4
Correlation analysis between BMI and other variables.

		BMI
SBP	r	0,224*
	p	0,034
DBP	r	0,252*
	p	0,015
IOP	r	0,212
	p	0,052
CCT	r	0,192
	p	0,067
GCL+IPL thickness	r	−0,122
	p	0,239
Macular thickness	r	−0,070
	p	0,501
Average RNFLT	r	−0,090
	p	0,386
Superior RNFLT	r	0,009
	p	0,930
Nasal RNFLT	r	−0,063
	p	0,543
Inferior RNFLT	r	−0,102
	p	0,326
Temporal RNFLT	r	−0,006
	p	0,956
BMO	r	−0,112
	p	0,287
LCD	r	0,172
	p	0,178
LCT	r	0,142
	p	0,266
PPCT T500	r	0,018
	p	0,866
PPCT T1000	r	−0,070
	p	0,498
PPCT T1500	r	−0,137
	p	0,185
PPCT N500	r	−0,200
	p	0,052
PPCT N1000	r	−0,247*
	p	0,016
PPCT N1500	r	−0,277*
	p	0,007
PPCT S500	r	−0,078
	p	0,455
PPCT S1500	r	−0,251*
	p	0,014
PPCT I500	r	−0,016
	p	0,881
PPCT I1000	r	−0,136
	p	0,190
PPCT I1500	r	−0,066
	p	0,528
SFCT	r	−0,086
	p	0,410
MCT T500	r	−0,122
	p	0,237
MCT T1000	r	−0,136
	p	0,190
MCT T1500	r	−0,172
	p	0,096
MCT N500	r	−0,087
	p	0,401
MCT N1000	r	−0,053
	p	0,613
MCT N1500	r	0,000
	p	0,998

SBP: systolic blood pressure; DBP: diastolic blood pressure; IOP: intraocular pressure; CCT: central corneal thickness; GCL+IPL: ganglion cell layer+inner plexiform layer; RNFLT: retinal nerve fiber layer thickness; BMO: Bruch's membrane opening; LCD: lamina cribrosa depth; LCT: lamina cribrosa thickness; PPCT T: temporal peripapillary choroidal thickness, PPCT N: nasal peripapillary choroidal thickness, PPCT S: superior peripapillary choroidal thickness; PPCT I: inferior peripapillary choroidal thickness; SFCT: subfoveal choroidal thickness, MCT T: temporal macular choroidal thickness; MCT N: nasal macular choroidal thickness.

The r value was obtained with the Pearson correlation coefficient for quantitative variables.

* $p<0.05$: statistically significant.

4. Discussion

In our study, we examined LC structure and microvascular changes in obese women using comprehensive OCT assessments of the posterior ocular region. We intended to investigate the pathogenesis of common ocular diseases associated with obesity, especially glaucoma. To the best of our knowledge, this study is the first in the literature to evaluate PPCT and LC in obesity.

The choroid is the main vascular component of the eye and is responsible for the blood circulation of the retinal outer layers and ONH. It serves several crucial functions, which include regulating IOP and thermoregulation in addition to delivering oxygen, nutrients, and waste removal for the ocular tissues [25]. As the retina and optic nerve lack an autonomic nervous system, they are severely influenced by vascular alterations [25]. Inadequate blood flow can lead to ischemia in the retina and optic nerve, resulting in a variety of ocular diseases [26–29].

Many investigations have revealed that obesity increases IOP, SBP, DBP, and the risk of glaucoma development [9,10,11,30]. In several studies on bariatric surgery, it has been reported that weight loss reduces IOP, SBP, and DBP in obese patients [31–33]. Posarelli et al. [33] stated that weight loss following bariatric surgery reduced CCT in addition to IOP, SBP, and DBP. We also found higher IOP and CCT in the obese group, in accordance with previous studies. In our study, we observed that SBP and DBP were also slightly higher in the obese group, although this was not statistically significant. We believe that it is related to the number of patients in our study. However, BMI was found to be significantly positively correlated with SBP and DBP in our study. Based on these findings, our study confirmed that obesity increases the risk of developing glaucoma, and hypertension as a consequence of a rise in IOP, SBP, and DBP.

Several studies in the literature have reported thinning in PPCT in a variety of diseases, including glaucoma, diabetes mellitus, and multiple sclerosis, and claimed that alterations in PPCT occur even prior to significant ocular involvement [34–36]. In the current study, which we conducted to investigate the mechanisms underlying ocular diseases in obesity, we discovered statistically significant thinning in the PPCT N1000, PPCT N1500, PPCT S1500, and PPCT T1500 of obese patients. PPCT I1000 and PPCT T1000 were also found to be slightly thinner in the obese group, although it was not statistically significant. This thinning of the choroidal layer surrounding the ONH indicates that obese patients have a microvascular perfusion problem and ischemia in the eye. It has been reported that vasoconstrictor substances such as endothelin-1 and vasopressin increase systemic circulation in obesity [12]. In addition, it has been stated that the level of nitric oxide, which is an essential vasodilator derived from endothelium, decreases in obese individuals and the balance between vasoconstrictor and vasodilator substances is disturbed [12,13]. Our study findings suggest that these increased vasoconstrictions also affect the eye and cause ischemia in ONH, which is a predictor for glaucoma development in particular.

The research examining MCT in obese patients in the literature had conflicting results. In some of these studies, MCT was thinner in the obese group than the normal-weight control group [37–39]; in other studies, MCT was thicker in the obese group [40,41], and in others, there was no substantial difference in MCT between the obese and healthy groups [42]. In these studies, only MCT was assessed; PPCT was not evaluated in any of them. The contradictory findings in MCT assessment may be attributable to sample sizes, age, gender, BMI levels, obesity duration, and concurrent ocular or systemic diseases. In our seven-region MCT analysis, we found no statistically significant differences between the obese group and the control group. The results of our study indicate that PPCT is affected by obesity before MCT changes. The thinning of PPCT may be followed by a subsequent alteration in MCT as the duration of obesity increases.

Some studies in the literature have indicated a thinning in LCT and an increase in LCD in diseases such as glaucoma, migraine, and Parkinson's disease [20,21,43]. But we found no significant differences in BMO, LCD, or LCT between the obese and the control group. These findings suggest that the triggering mechanism in glaucoma caused by obesity is microvascular abnormalities in the peripapillary region rather than structural changes in the LC.

The most significant limitation of our investigation is that we did not assess the duration of obesity. This is the first study to examine PPCT and LC structure in obese patients. Further research with larger populations and attention to the duration of obesity is required to confirm our findings.

As a consequence, our study is the first to evaluate PPCT and LC structure in addition to MCT in obese patients. Obese patients revealed statistically significant thinning in the PPCT N1000, PPCT N1500, PPCT S1500, and PPCT T1500 compared to the control group, whereas there was no statistically significant difference in BMO, LCD, LCT, or MCT. In addition, obese patients had higher IOP, and CCT. The microvascular disorder, which we discovered in the outer zone of the peripapillary region, indicates impaired blood flow in ONH, even in obese individuals who have not yet developed any ocular disease. Our findings suggest that microvascular alteration in the peripapillary region may be the initial event in the pathogenesis of many obesity-related ocular diseases, particularly glaucoma.

Funding

This research did not receive any specific grants from funding agencies in the public, commercial, or not-for-profit sectors.

CRediT authorship contribution statement

Sumeyra Koprubasi: Writing – review & editing, Writing – original draft, Supervision, Project administration, Methodology, Investigation, Formal analysis, Data curation, Conceptualization. **Erkan Bulut:** Writing – review & editing, Supervision, Data curation.

Declaration of Competing Interest

Each author declared that there was no conflict of interest in this study.

References

[1] A. Berghöfer, T. Pischon, T. Reinhold, C.M. Apovian, A.M. Sharma, S.N. Willich, Obesity prevalence from a European perspective: a systematic review, BMC Public Health 8 (2008) 200, https://doi.org/10.1186/1471-2458-8-200.

[2] Collaboration N.R.F, Trends in adult body-mass index in 200 countries from 1975 to 2014: a pooled analysis of 1698 population-based measurement studies with 19.2 million participants, Lancet 387 (10026) (2016) 1377–1396, https://doi.org/10.1016/S0140-6736(16)30054-X.

[3] A.M. Jonk, A.J. Houben, R.T. de Jongh, E.H. Serné, N.C. Schaper, C.D. Stehouwer, Microvascular dysfunction in obesity: a potential mechanism in the pathogenesis of obesity-associated insulin resistance and hypertension, Physiology (Bethesda) 22 (2007) 252–260, https://doi.org/10.1152/physiol.00012.2007.

[4] G.M. Singh, G. Danaei, F. Farzadfar, G.A. Stevens, M. Woodward, D. Wormser, et al., The age-specific quantitative effects of metabolic risk factors on cardiovascular diseases and diabetes: a pooled analysis, PLoS One 8 (7) (2013) e65174, https://doi.org/10.1371/journal.pone.0065174.

[5] B. Lauby-Secretan, C. Scoccianti, D. Loomis, Y. Grosse, F. Bianchini, K. Straif, Body fatness and cancer-viewpoint of the IARC working group, NEJM 375 (8) (2016) 794–798, https://doi.org/10.1056/NEJMsr1606602.

[6] N. Cheung, T.Y. Wong, Obesity and eye diseases, Surv. Ophthalmol. 52 (2) (2007) 180–195, https://doi.org/10.1016/j.survophthal.2006.12.003.

[7] A.G. Tan, A. Kifley, V.M. Flood, E.G. Holliday, R.J. Scott, R.G. Cumming, et al., Evaluating the associations between obesity and age-related cataract: a Mendelian randomization study, Am. J. Clin. Nutr. 110 (4) (2019) 969–976, https://doi.org/10.1093/ajcn/nqz167.

[8] Age-Related Eye Disease Study Research Group, Risk factors associated with age-related nuclear and cortical cataract: a case-control study in the age-related eye

disease study, AREDS report no.5, Opthalmology 108 (8) (2001) 1400–1408, https://doi.org/10.1016/S0161- 6420(01)00626-1.
[9] P. Gasser, D. Stumpfig, A. Schotzau, U. Ackermann-Liebrich, J. Flammer, Body mass index in glaucoma, J. Glaucoma 8 (1) (1999) 8–11, https://doi.org/10.1097/00061198-199902000-00004.
[10] Y. Jung, G.N. Kim, E.B. Oh, K. Ohn, J.I. Moon, Metabolic health, obesity, and intraocular pressure, J. Clin. Med. 12 (5) (2023) 2066, https://doi.org/10.3390/jcm12052066.
[11] R. Karadag, Z. Arslanyilmaz, B. Aydin, I.F Hepsen, Effects of body mass index on intraocular pressure and ocular pulse amplitude, Int. J. Ophthalmol. 5 (5) (2012) 605–608, https://doi.org/10.3980/j.issn.2222-3959.2012.05.12.
[12] C. Ferri, C. Bellini, G. Desideri, R. Baldoncini, G. Properzi, A. Santucci, et al., Circulating endothelin-1 levels in obese patients with the metabolic syndrome, Exp. Clin. Endocrinol. Diabetes 105 Suppl 2 (1997) 38–40, https://doi.org/10.1055/s-0029-1211794.
[13] G.A. Cioffi, S. Orgul, E. Onda, D.R. Bacon, E.M. Van Buskirk, An in vivo model of chronic optic nerve ischemia: the dose-dependent effects of endothelin-1 on the optic nerve microvasculature, Curr. Eye Res. 4 (12) (1995) 1147–1153, https://doi.org/10.3109/02713689508995821.
[14] L. Wang, C.F. Burgoyne, G. Cull, S. Thompson, B. Fortune, Static blood flow autoregulation in the optic nerve head in normal and experimental glaucoma, Investig. Ophthalmol. Vis. Sci. 55 (2) (2014) 873–880, https://doi.org/10.1167/iovs.13-13716.
[15] A.S. Hafez, R.L. Bizzarro, M.R. Lesk, Evaluation of optic nerve head and peripapillary retinal blood flow in glaucoma patients, ocular hypertensives, and normal subjects, Am. J. Ophthalmol. 136 (6) (2003) 1022–1031, https://doi.org/10.1016/s0002-9394(03)00632-9.
[16] J.Y. You, S.C. Park, D. Su, C.C. Teng, J.M. Liebmann, R. Ritch, Focal lamina cribrosa defects associated with glaucomatous rim thinning and acquired pits, JAMA Ophthalmol. 131 (3) (2013) 314–320, https://doi.org/10.1001/jamaophthalmol.2013.1926.
[17] M.D. Roberts, V. Grau, J. Grimm, J. Reynaud, A.J. Bellezza, C.F. Burgoyne, et al., Remodeling of the connective tissue microarchitecture of the lamina cribrosa in early experimental glaucoma, Investig. Ophthalmol. Vis. Sci. 50 (2) (2009) 681–690, https://doi.org/10.1167/iovs.08-1792.
[18] B.C. Chauhan, N. O'Leary, F.A. AlMobarak, A.S.C. Reis, H. Yang, G.P. Sharpe, et al., Enhanced detection of open-angle glaucoma with an anatomically accurate optical coherence tomography–derived neuroretinal rim parameter, Ophthalmology 120 (3) (2013) 535–543, https://doi.org/10.1016/j.ophtha.2012.09.055.
[19] C.D. Fryar, M.D. Carroll, J. Afful, Prevalence of overweight, obesity, and Severe Obesity Among Adults Aged 20 and over: United States, 1960–1962 Through 2017–2018, NCHS Health E-Stats, Centers for Disease Control and Prevention, 2020. Updated February 8, 2021. Accessed January 29, 2021, www.cdc.gov/nchs/data/hestat/obesity-adult-17-18/obesity-adult.htm.
[20] H.Y.L. Park, S.H. Jeon, C.K. Park, Enhanced depth imaging detects lamina cribrosa thickness differences in normal tension glaucoma and primary open-angle glaucoma, Ophthalmology 119 (1) (2012) 10–20, https://doi.org/10.1016/j.ophtha.2011.07.033.
[21] E. Sirakaya, B. Kucuk, A. Agadayi, N. Yilmaz, Evaluation of the lamina cribrosa thickness and depth in patients with migraine, Int. Ophthalmol. 40 (1) (2020) 89–98, https://doi.org/10.1007/s10792-019-01160-2.
[22] E.J. Lee, T.W. Kim, H. Kim, S.H. Lee, M.J.A. Girard, J.M. Mari, Comparison between lamina cribrosa depth and curvature as a predictor of progressive retinal nerve fiber layer thinning in primary open angle glaucoma, Ophthalmol. Glaucoma 1 (2018) 44–51, https://doi.org/10.1016/j.ogla.2018.05.007.
[23] J.A. Kim, T.W. Kim, E.J. Lee, M.J.A. Girard, J.M. Mari, Lamina cribrosa morphology in glaucomatous eyes with hemifield defect in a Korean population, Ophthalmology 126 (2019) 692–701, https://doi.org/10.1016/j.ophtha.2018.12.042.
[24] M. Balasubramanian, C. Bowd, G. Vizzeri, R.N. Weinreb, L.M. Zangwill, Effect of image quality on tissue thickness measurements obtained with spectral-domain optical coherence tomography, Opt. Express 17 (5) (2009) 4019–4036, https://doi.org/10.1364/oe.17.004019.
[25] D.L. Nickla, J. Wallman, The multifunctional choroid, Prog. Retin. Eye Res. 29 (2) (2010) 144–168, https://doi.org/10.1016/j.preteyeres.2009.12.002.
[26] C.Y. Cheung, M.K. Ikram, C. Sabanayagam, T.Y. Wong, Retinal microvasculature as a model to study the manifestations of hypertension, Hypertension 60 (5) (2012) 1094–1103, https://doi.org/10.1161/HYPERTENSIONAHA.111.189142.
[27] Y. Ruan, S. Jiang, A. Gericke, Age-related macuar degeneration: role of oxidative stress and blood vessels, Int. J. Mol. Sci. 22 (3) (2021) 1296, https://doi.org/10.3390/ijms22031296.
[28] W. Wang, S. Liu, Z. Qiu, M. He, L. Wang, Y. Li, et al., Choroidal thickness in diabetes and diabetic retinopathy: a swept source OCT study, Investig. Ophthalmol. Vis. Sci. 61 (4) (2020) 29, https://doi.org/10.1167/iovs.61.4.29.
[29] I. Goharian, M. Sehi, Is there any role for the choroid in glaucoma? J. Glaucoma 25 (5) (2016) 452–458, https://doi.org/10.1097/IJG.0000000000000166.
[30] M. Yoshida, M. Ishikawa, K. Karita, A. Kokaze, M. Harada, S. Take, et al., association of blood pressure and body mass index with intraocular pressure in middle-aged and older japanese residents: a cross-sectional and longitudinal study, Acta Med. Okayama 68 (1) (2014) 27–34, https://doi.org/10.18926/AMO/52141.
[31] Z. Burgansky-Eliash, A. Achiron, I. Hecht, M Shimonov, Reduction of intraocular pressure after bariatric surgery, Acta Ophthalmol. 96 (5) (2018) e592–e595, https://doi.org/10.1111/aos.13722.
[32] A. Viljanen, J.C. Hannukainen, M. Soinio, H.K. Karlsson, P. Salminen, P. Nuutila, The effect of bariatric surgery on intraocular pressure, Acta Ophthalmol. 96 (8) (2018) 849–852, https://doi.org/10.1111/aos.13826.
[33] C. Posarelli, G. Salvetti, P. Piaggi, F. Guido, G. Ceccarini, F. Santini, et al., Ophthalmologic evaluation of severely obese patients undergoing bariatric surgery: a pilot, monocentric, prospective, open-label study, PLoS One 14 (5) (2019), e0216351, https://doi.org/10.1371/journal.pone.0216351.
[34] Z. Lin, S. Huang, B. Xie, Y. Zhong, Peripapillary choroidal thickness and open-angle glaucoma: a meta-analysis, J. Ophthalmol. 2016 (2016), 5484568, https://doi.org/10.1155/2016/5484568.
[35] B.C. Ermerak, O. Yalcinbayir, E. Eren, E. Sobu, C. Erseven, A.A. Yucel, Evaluation of choroidal thickness in children with type 1 diabetes: the role of optical coherence tomography in diabetic retinopathy screening, Clin. Pediatr. Endocrinol. 30 (1) (2021) 41–47, https://doi.org/10.1297/cpe.30.41.
[36] E. Garcia-Martin, L. Jarauta, L.E. Pablo, M.P. Bambo, J.R. Ara, J. Martin, et al., Changes in peripapillary choroidal thickness in patients with multiple sclerosis, Acta Ophthalmol. 97 (1) (2019) e77–e83, https://doi.org/10.1111/aos.13807.
[37] I. Yilmaz, A. Ozkaya, M. Kocamaz, S. Ahmet, H.M. Ozkaya, D. Yasa, et al., Correlation of choroidal thickness and body mass index, Retina 35 (10) (2015) 2085–2090, https://doi.org/10.1097/IAE.0000000000000582.
[38] B. Dogan, E.M. Kazim, U. Dogan, M. Habibi, N. Bulbuller, C.D. Turgut, et al., The retinal nerve fiber layer, choroidal thickness, and central macular thickness in morbid obesity: an evaluation using spectral-domain optical coherence tomography, Eur. Rev. Med. Pharmacol. Sci. 20 (5) (2016) 886–891.
[39] H. Öncül, M. Çaglayan, M. Fuat Alakus, F.Y. Öncül, U. Dag, E. Arac, et al., Evaluation of the subfoveal choroidal and outer retinal layer thickness in obese women, Clin. Exp. Optom. 104 (2) (2021) 178–186, https://doi.org/10.1111/cxo.13108.
[40] E. Yumusak, K. Ornek, S.A. Durmaz, A. Cifci, H.A. Guler, Z. Bacanli, Choroidal thickness in obese women, BMC Ophthalmol. 16 (1) (2016) 48, https://doi.org/10.1186/s12886-016-0227-z.
[41] A.D. Bulus, M.E. Can, A. Baytaroglu, G.D. Can, H.B. Cakmak, N. Andiran, Choroidal thickness in childhood obesity, Ophthal. Surg. Lasers Imaging Retina 48 (1) (2017) 10–17, https://doi.org/10.3928/23258160-20161219-02.
[42] N. Panon, K. Luangsawang, C. Rugaber, T. Tongchit, N. Thonsepee, D. Cheaha, et al., Correlation between body mass index and ocular parameters, Clin. Ophthalmol. 13 (2019) 763–769, https://doi.org/10.2147/OPTH.S196622.
[43] M. Eraslan, E. Cerman, S. Yildiz Balci, H. Celiker, O. Sahin, A. Temel, et al., The choroid and lamina cribrosa is affected in patients with Parkinson's disease: enhanced depth imaging optical coherence tomography study, Acta Ophthalmol. 94 (1) (2016) e68–e75, https://doi.org/10.1111/aos.12809.